

S.E.A.S

Self Embedding Anchor System

University of New Hampshire
Ocean Projects TECH 797

Team Members

Douglas Flanders – Mechanical Engineering
Keith Hnatow – Mechanical Engineering
Zachary Voydach – Mechanical Engineering
Eric Fergusson – Mechanical Engineering

Project Advisor

Dr. Barbaros Celikkol

UNIVERSITY OF NEW HAMPSHIRE



Abstract

The anchoring systems used to secure many offshore structures conventionally employ multiple drag type anchors and considerably long, heavy chain. By reducing the amount of equipment needed to secure offshore structures, installation, maintenance and labor costs could be reduced. One solution to this problem is to use a single point, vertical lift mooring system utilizing a hydro-jet anchor. Installation of this type of anchor is accomplished by employing a tripod support system that can be retrieved and reused. Test results show that hydro-jet anchors perform best in sandy sediments. The anchors developed have a holding capacity to weight ratio of approximately twenty-five to one.

Acknowledgements

This work is the result of research sponsored in part by the National Sea Grant College Program, NOAA, Department of Commerce, under grant #NA96RG0102 through the University of New Hampshire/University of Maine Sea Grant College Program.

We would like to extend our thanks to those individuals who contributed to the success of SEAS:

Professor Barbaros Celikkol

Professor Pedro de Alba

Noel Carlson

Captain Paul Pelletier

Captain Ken Houtler

Liz Kintzing

Mike Lombardi

Jon Scott

Paul Lavoie

Anne Stork

and the people of the Center for Ocean Engineering

Table of Contents

	<u>Page Number</u>
Abstract	1
Acknowledgements	2
Introduction	7
Overview	7
Direct Embedment Anchors	7
Hydro-Jet Direct Embedment Anchor	8
Tripod Support Structure	8
System Operation	8
Timeline	10
Budget	13
Design Description	14
Overview	14
Preliminary Anchor Designs	14
Final Anchor Design	16
Cone Anchor	16
Pyramid Anchor	17
Preliminary Support Structure Design	18
Force Application	19
Release Mechanism	21
Final Tripod Support Structure	23
Testing and Evaluation	25
Anchor Testing	25
Tripod Testing	27
Results	31
Discussion	37
Summary	37
Future Testing	37

References.....	39
Appendix A: Theoretical holding capacity calculations.....	40
Appendix B: Pressure loss in water hose calculations.....	43

Table of Figures

	<u>Page Numbers</u>
Figure 1: Overall system.....	9
Figure 2: Preliminary screw anchor design.	15
Figure 3: Preliminary self-propelled, expanding anchor design.	15
Figure 4: Initial cone anchor design used to demonstrate the hydro-jet principle.....	16
Figure 5: Three rigid pyramid anchors of varying size used in the testing process.....	17
Figure 6: The Kevlar folding anchor.	18
Figure 7: Tripod shown with the insertion pole.....	19
Figure 8: Tripod and anchor with springs attached to the insertion pole.....	20
Figure 9: Tripod with a large weight on the top of the insertion pole.	21
Figure 10: Tripod with swing release mechanism before engagement.....	22
Figure 11: Tripod with swing mechanism after engagement.....	22
Figure 12: Spring, pin, and flapper release mechanism.....	23
Figure 13: Final tripod design with anchor and release mechanism shown.	24
Figure 14: Map of test sites one, three, four, and five in Portsmouth harbor	26
Figure 15: Second test site at the Isle of Shoals.....	28
Figure 16: The anchor failed to embed itself after ten minutes of pumping water.....	29
Figure 17: Anchor insertion process completed.	30
Figure 18: The resulting backfill of the sediment after a rest period of twenty minutes.....	30
Figure 19: Theoretical uplift capacity versus anchor embedment depth.	32
Figure 20: Theoretical uplift capacity versus weight of anchors in air.....	34
Figure 21: Actual uplift capacity versus weight of anchors in air.	34
Figure 22: Theoretical uplift capacity versus anchor base area.	35
Figure 23: Actual uplift capacity versus anchor base area.	36

List of Tables

	<u>Page Number</u>
Table 1: Timeline for the development of the Self Embedding Anchor System.....	11
Table 2: Proposed and actual budget for the Self Embedding Anchor System.....	13
Table 3: Dimensions of the four fabricated anchors.....	18
Table 4: Relative successful embedding of the anchors in different sediments.....	31
Table 5: Experimental results of the anchor pull tests.....	33
Table 6: Theoretical and actual holding capacity to weight ratios.....	33

Introduction

Overview

Mooring of offshore structures is currently an expensive and labor-intensive process. Conventionally, multiple anchors are used to secure many large offshore structures. These anchors require large amounts of equipment and personnel to be installed. Such anchor systems also have relatively large residual costs. For example, the area of the sea floor taken up by the projected area of the offshore structure must be leased. By reducing the amount of equipment needed to secure offshore structures, installation, maintenance and labor costs could be reduced. A directly inserted mooring system would greatly reduce the projected area of the offshore structure, therefore, reducing the overall cost of the anchor system. This alternative anchor system should be designed with ease of installation as one of the goals. The design should be light enough to be handled on a boat deck and should install itself in the sea floor without the aid of divers. It was decided that the only anchor type that could meet this requirement is a direct embedment anchor.

Direct Embedment Anchors

Direct embedment anchors are inserted vertically into the sediment and derive their holding capacity based on the type of sediment and depth of insertion. They are designed to resist vertical loads. Direct insertion anchors range in holding capacity from small, diver-installed anchors with load capacities of one to ten thousand pounds to larger capacities of one hundred fifty thousand pounds.

There are several types of direct embedment anchors, each utilizing different techniques for insertion. Some are inserted using a propellant and are essentially fired into the sediment. Others are inserted into place using a hydraulic hammer. Another type of direct embedment anchor uses a water jet to disturb the sediment, basically drilling a hole allowing the anchor to be inserted. This is the type of anchor that will be developed for this project. It meets the requirements of ease of installation with a minimum of equipment. The only required special equipment will be a pump to supply the water jet and an insertion system to install the anchor without the aid of personnel.

Hydro-Jet Direct Embedment Anchor

Hydro-jet anchors function best in sands that are easily liquefied. After the disturbance period of jetting-in the anchor, the sediment returns to a more dense condition over the anchor. The use of hydro-jet anchors in other sediments is not recommended. Installation in clay sediments is not as easily accomplished and the resulting backfill is much weaker than the undisturbed sediment. In hard clay or cobble stone sediments, installation is very slow and uneconomical.

Tripod Support Structure

The tripod support structure is unique to this project. In order to remotely insert direct embedment anchors a structure is required to carry the anchor to the sea floor, provide a stable platform for the anchor to be inserted, insert the anchor, and provide visual notification of a successful insertion process.

System Operation

The overall anchor and insertion system is shown in Figure 1. An eight horsepower pump provides the driving force, the water jet. The pump is capable of supplying twenty-five gallons a minute at a pressure of two hundred pounds per square inch. The supply for the jet is drawn from the ocean through a two-inch inner diameter hose. The hose is ten feet long and has a check valve attached to one side to aid in keeping the pump primed. The pump outlet is connected to one hundred feet of inch and a half high-pressure hose. The other end of the hose is attached to the tripod insertion pole. The hose connects with the pipe that is used to drive the anchor into the sediment. All hoses are connected using quick disconnect couplings. The pipe, anchor, and tripod are coupled together through a pin release mechanism. Once the water is activated the release mechanism triggers. This allows the pipe to provide a constant force to the anchor as the water jet burrows a hole. A collar affixed to the pipe restricts the insertion pole from driving the anchor further when the anchor is inserted to the correct depth. This collar also triggers the release of a ball float. When the ball float reaches the surface, the operator knows to shut the engine down. At this point the tripod is raised to the surface without the anchor.

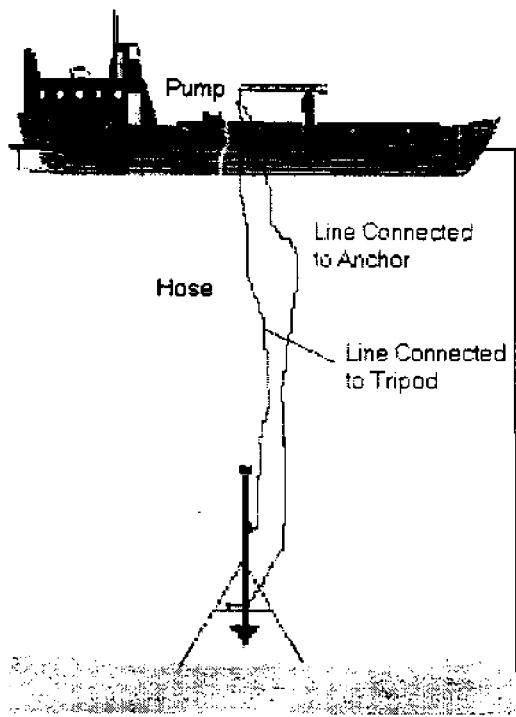


Figure 1: Overall system.

Timeline

The development of the anchors and support structure plus testing of all apparatus was to be completed in eight months. Table 1 shows the project timeline – proposed and actual time accomplishments.

The design process, theoretical calculations, anchor assembly, and testing began early since it was determined that a preliminary cone shaped anchor should be tested immediately to prove the hydro-jet concept. The experience gained from the preliminary design, manufacturing and testing would prove useful in subsequent stages of design and implementation.

The design process required more time than was planned. The extended design time was attributed to the design of the tripod support structure, explicitly the release mechanism. This pushed off the testing time until late March, early April. In addition, the testing time was pushed back due to the availability of the *R/V Gulf Challenger* and diver scheduling.

Table 1: Timeline for the development of the Self Embedding Anchor System.

Task	September '99	October '99	November '99	December '99	January '00	February '00	March '00	April '00	May '00
Literature Search									
Design Process									
Theoretical Calculations									
Order Materials									
Anchor Assembly									
Tripod Assembly									
Test Preparations									
Testing									
Data Analysis									
Report Writing									
Oral Report									

Legend

- Planned and accomplished.
- Planned but not accomplished.
- Additional time required.

Budget

The project was allotted \$2000 for the design, construction, and testing of the support tripod and anchors. Table 2 shows the planned budget for the project and the actual cost of each item. Ultimately, the budget goals were met. A few items were not budgeted, some items went over budget, and others came in below budget. For example, the cost of the hose and couplings was more expensive than was planned. The lift bag was not used in the testing process, therefore, saving approximately \$300. The actual cost of the raw materials was much less than expected since steel was the primary material used in the construction of the anchors and tripod.

Table 2: Proposed and actual budget for the Self Embedding Anchor System.

Item	Budgeted	Actual Cost
Raw Materials (anchor, tripod, hardware)	\$400	\$164.21
Fabrication	\$800	\$708
Hose & Couplings	\$150	\$358.44
Rope	\$50	N/C
Gas Tank & Hose	\$0	\$24.95
Lift Bag – one day (rental)	\$100/day	Not Used
<i>R/V Gulf Challenger</i>	\$500	\$555
Photographic Supplies	\$0	\$18
Total	\$2000	\$1828.60

Design Description

Overview

Several anchor and support structure designs were considered before achieving the final product. The anchor design had to incorporate the hydro-jet principle either as a way to disturb the sediment or use it for propulsion. Initially, they were to be self-supportive. They were to be designed such that they could be inserted without the aid of a support structure. In addition, the anchors required a high holding capacity to weight ratio.

It was later determined that in order to meet the requirements of inserting the anchors a structure was needed to aid in the insertion process. The requirements of the support structure were that it had to deliver the anchor to the sea floor, maintain a stable platform for inserting the anchor, ensure the anchor was inserted vertically, regulate the embedment depth of the anchors, provide visual notification of the completion of the insertion process, and be reusable.

Initial anchor designs applied the availability of the water jet to propel the anchor into the sediment as well using the jet to dig a hole for the anchor. However, such designs required a very high performance pump. In addition, manufacturing costs were high.

The shape of the support structure was a bit trivial, however, the mechanisms required to perform the needed operations were not. The tripod shape provides the required stability and is cost effective. A couple mechanisms to initiate the anchor insertion process were considered. Ultimately, a simple, small design was chosen for its ease of manufacturing and implementation.

Preliminary Anchor Designs

Figure 2 details the first of the preliminary anchor designs. It is conical in shape with threads on its outer shell that act as a screw. The shank of the anchor is hollow. Two small diameter pipes extend from the shank that act to divert some of the water flow to provide an external torque on the system. In theory part of the water would flow out the tip of the anchor to disperse the sediment and the rest of the water flow would shoot out of angled jets (perpendicular to the perimeter of the top of the cone) pushing the anchor down and twisting it into the sediment. This would be a strong, compact anchor whose uplift capacity would result not only from the sediment failure surface due to the projected area of the cone, but also from the sediment failure surface due to the threads.

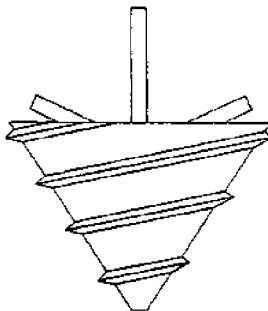


Figure 2: Preliminary screw anchor design.

The major problem with this design is that the force of water jets would not be strong enough to push and twist the anchor into the sediment. The flow loss required to twist the anchor would result in poor liquification of the sediment. A better pump might remedy this issue; however, such a pump would be expensive and is not in the scope of the project. A second drawback from this design is that the towline and water hose would have to be decoupled from the anchor to allow the anchor to twist. Additionally, this type of anchor would be expensive to fabricate because of the threads on the cone and the water jets.

A second preliminary anchor design operates on similar principles as the first. The design is a self-propelled expanding anchor shown in Figure 3. The anchor folds into a more compact form during the insertion process, but is unfolded into a conical shape after it is embedded. In theory, part of the water flow would flow out the tip of the folded anchor to disperse the sediment and the rest of the water flow would shoot out of the top of the anchor; providing a thrust force to push the anchor into the sediment. When the sediment had resettled, the anchor would be keyed into position by applying a load. This would allow the anchor to utilize more undisturbed sediment as compared to a non-folding anchor. This anchor would have a higher holding capacity than a similar sized anchor because it disturbs less sediment and thus leaving sediment with more natural, stronger shear properties.

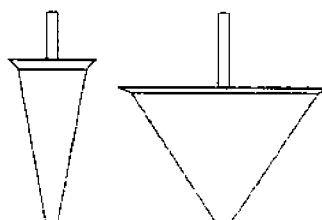


Figure 3: Preliminary self-propelled, expanding anchor design.

The major problem with this design is that the required thrust force of water jet would not be great enough to insert the anchor. Again, the flow loss due to the thrust force would reduce the effectiveness of liquefying the sediment. Another major drawback of this design is that it might not insert itself vertically into the sediment. Plus, the external thrust force could cause it to fall over. The reliability of the anchor keying open is also a question. It might not open properly and possibly require a deeper embedment depth to accommodate for opening.

Final Anchor Design

After considering the above designs, it was determined that the design of a completely self-supportive, self-embedding anchor could not be accomplished. A separate structure is required to assist in the embedment process. Therefore, the final anchor designs incorporate the use of a support structure.

Cone Anchor

Figure 4 shows the initial conical shaped fabricated anchor. This anchor was built early in the progression of the project primarily to prove and demonstrate the concept of hydro-jet anchors. The cone has a height of twelve inches and an upper diameter of twelve inches. The cone is constructed from sixteenth of inch thick steel that was rolled into shape. The end of the cone is welded to a one inch threaded pipe coupling. The shank of the anchor is one inch in diameter and five feet long. The shank screws into the coupling. Steel wire was wound from the cone to the shank to provide support from folding.

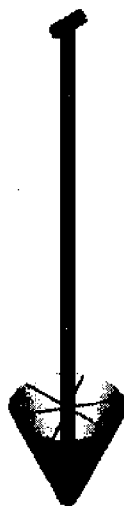


Figure 4: Initial cone anchor design used to demonstrate the hydro-jet principle.

Pyramid Anchor

Due to the manufacturing cost of the preliminary cone anchor, it was determined that a pyramid shaped anchor would be as successful as a cone, but cost considerably less to fabricate. Three anchors of varying dimensions were produced and are shown in Figure 5. Table 3 shows the dimensions of each anchor. In addition, a folding anchor was produced to compare its uplift capacity to that of a rigid anchor of the same dimensions. Figure 6 shows the folding anchor design. The frame and hardware are steel and the web is Kevlar.



Figure 5: Three rigid pyramid anchors of varying size used in the testing process.



Figure 6: The Kevlar folding anchor.

Table 3: Dimensions of the four fabricated anchors.

Anchor	Type	Height (in)	Base Length (in)	Base Area (ft ²)	Weight (lbf)
Small	Rigid	2	2	8.5	10.1
Medium	Rigid	6	6	10.5	13.3
Large	Rigid	12	12	14	21.7
Medium	Folding	6	6	10.5	16.5

Preliminary Support Structure Design

It was determined that a support structure would be required to aid the anchors in the insertion process because it was not feasible that water would be able to supply enough thrust to insert the anchors into the sediment and insert them vertically. The tripod was chosen as the basic shape for the support structure since it is the simplest structure that could provide a stable platform.

There are some issues to consider in designing the additional mechanisms of the support structure. First, the tripod needs to be large enough to execute its operation as well as easily maneuverable. The anchor and tripod need to be coupled to one another during the descent to the sea floor; however, need to be decoupled in order to retrieve the tripod. A release

mechanism is required to begin the insertion process after the tripod has landed on the sea bottom. The largest design consideration is to determine a system that will initiate the insertion process automatically. Lastly, the structure has to provide a constant force to the anchor to insert it into the sediment.

It was determined that a long pipe would be required to deliver the water jet to the anchor as shown in Figure 7. The tripod guides the pipe and ensures total vertical insertion of the anchor. The high-pressure water hose is connected to the top of the pole. The pipe is slightly larger in diameter than the shank of the anchor, therefore, allowing the shank to be inserted inside the pole. The water flows through the insertion pipe and through the anchor shank to disperse the sediment. The tripod supports the pole in two separate places and thus ensures purely vertical insertion of the anchor. Another advantage with using the pole is that the hose stays attached to the tripod.

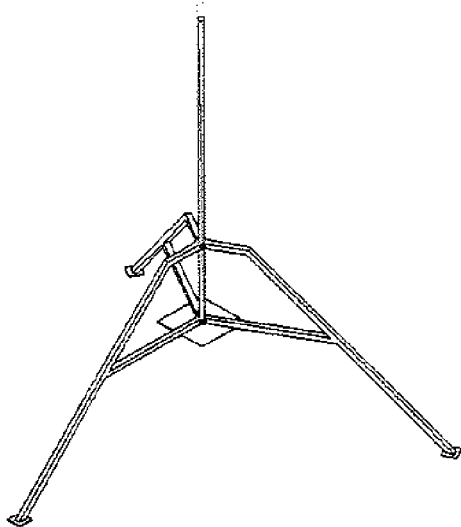


Figure 7: Tripod shown with the insertion pole.

Force Application

The anchor requires a constant applied force in order to be inserted into the sediment. One of the preliminary designs to provide this force uses springs attached to the tripod and the top of the insertion pole as shown in Figure 8. This design would be light and the amount of driving force could be easily and inexpensively adjusted by exchanging the springs for those with a different spring constant.

The major problem with using springs is that the driving force is not constant. The force decreases as the anchor is inserted deeper. To have adequate force to complete the insertion process requires very stiff springs. However, using springs with large spring constants would make setting the springs impossible to accomplish by hand. An additional problem with using springs is that they are more apt to rust and weaken.

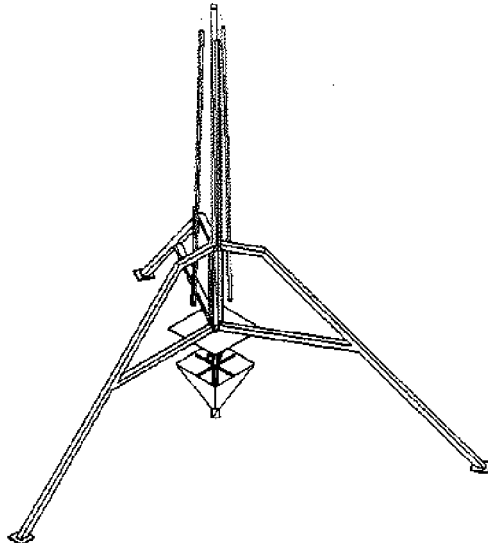


Figure 8: Tripod and anchor with springs attached to the insertion pole.

Another preliminary design incorporates a large mass at the top of the insertion pole shown in Figure 9. This would provide a constant driving force and is simple. The major problem with this design is that it makes the center of gravity very high. It also increases the weight of the tripod, thus reducing its maneuverability.

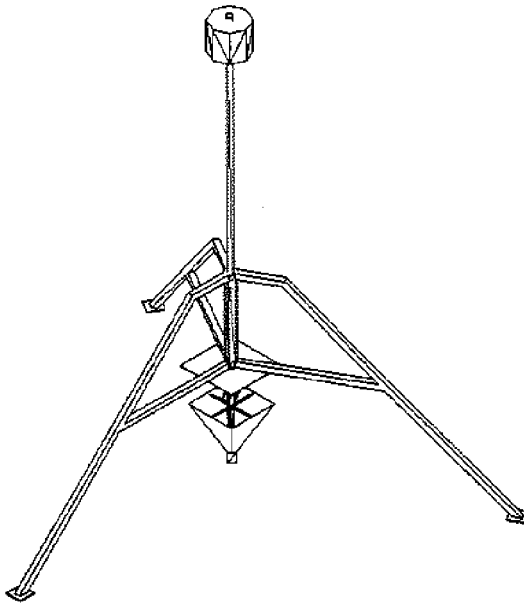


Figure 9: Tripod with a large weight on the top of the insertion pole.

A final design suggests using a heavy pole to insert the anchors. This design also provides a constant driving force, but is evenly distributed and does not affect the center of gravity. One downside of this design is that it increases the mass of the support structure.

Release Mechanism

The design of a mechanism that would release the insertion pole and anchor was considered. The function of the mechanism would be to couple the anchor to the tripod during the descent to the sea floor. Once the tripod stabilized, the mechanism would release the anchor and insertion pole to activate the insertion process.

A preliminary release design relies on a separate line that would connect to a pin holding up the insertion pole and anchor. The pin would be pulled from the surface after the tripod landed on the bottom. This design is simple and knowledge of the release would be evident since the pin would be retrieved. The major problem with this design was that it introduced another line in the water and if it tangled the pin could not be pulled out.

A release design, which relies on thrust from the water jet, is shown in Figure 10. Figure 11 shows the result after the swing mechanism was tripped and the insertion pole fully extended. A plate under the tip of the anchor holds the insertion pole and anchor with two supporting arms. A spring leading from the plate to one of the legs of the tripod provides a force to swing the plate

clear once the water pump was activated. A lip on the plate against the anchor provides a resistance so the plate would not be pulled out during the descent to the sea floor. Once the water was turned on the anchor and insertion pole would be forced up past the lip and the plate would be pulled clear allowing the anchor to fall and be inserted. The advantage of this design is that it trips only when the water is turned on. It also does not require any holes in the insertion pole.

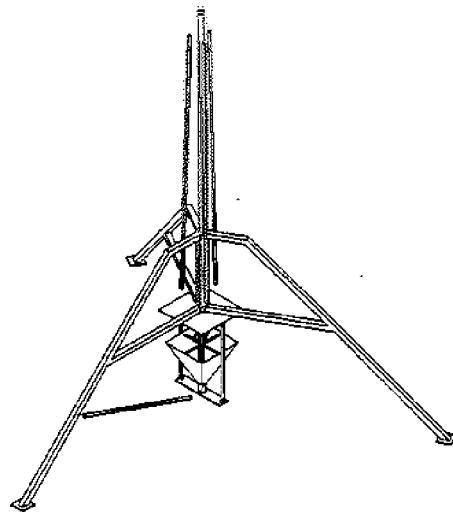


Figure 10: Tripod with swing release mechanism before engagement.

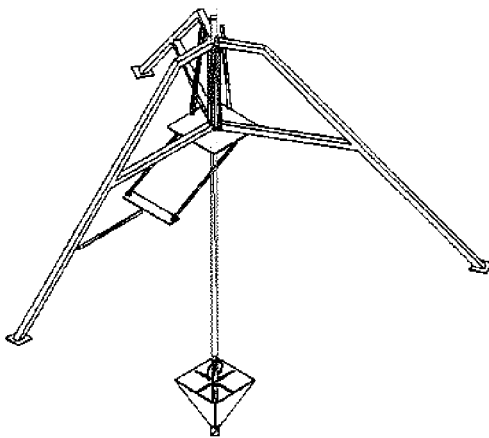


Figure 11: Tripod with swing mechanism after engagement.

There are many disadvantages to this design. Primarily, this design complicates the overall structure with the addition of members and a spring that could ultimately become fouled. The system could interfere with the anchor insertion. During descent, the tripod might encounter

a bounce or jarring that would cause premature release. Also it relies on the thrust of the water to be great enough to force the anchor and insertion pole vertically for an instant. Such a force is not reliably reproducible.

Further preliminary designs produced the flapper release shown in Figure 12. A spring-loaded pin couples with the insertion pole and anchor while another release pin holds the spring-loaded pin in place. The release pin is connected to an arm that has an attached flat plate. The flat plate is inserted through a cut in the side of the pole. When the water is turned on, the force on the plate is pushed down which thus pulls the release pin out allowing the spring-loaded pin to disengage from the anchor and insertion pole. The anchor and insertion pole are then allowed to fall to the sediment and begin the insertion process. The advantage of this design is that it is very compact and will not interfere with the insertion of the anchor. It also releases automatically when the water jet is activated. The disadvantage of this design is that it requires a substantial hole in the side of the insertion pole and thus increases the flow loss. Additionally, it relies on the force of the water to be great enough to force the flapper down.

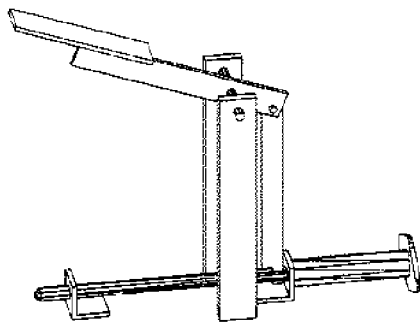


Figure 12: Spring, pin, and flapper release mechanism.

Final Tripod Support Structure

The finalized tripod support structure is shown in Figure 13. The heavy pole provides the insertion force. The flapper release mechanism is incorporated to couple the anchor with the tripod. It was determined that this system would produce the most efficient insertion of the anchors despite the flow loss due to the holes in the pole. The tripod frame is constructed from one-inch square stock steel. The plate at mid span and footplates are eighth-inch steel. The release mechanism is constructed from steel as well. The tripod weighs forty-seven pounds and the pole weighs thirty-five pounds.

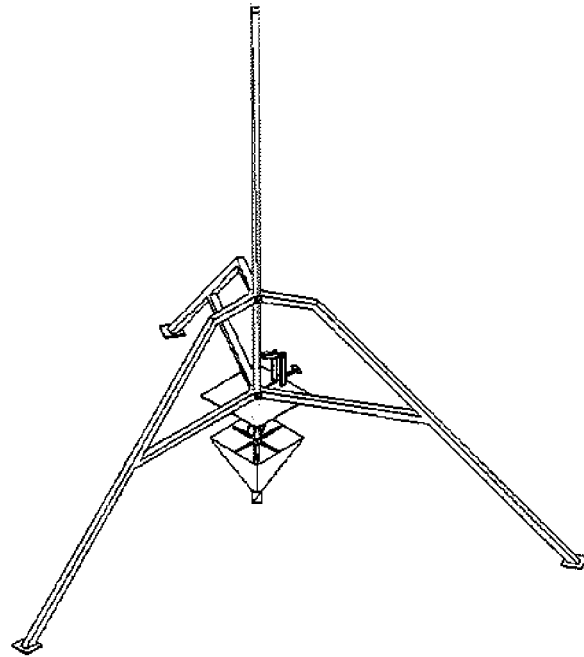


Figure 13: Final tripod design with anchor and release mechanism shown.

Testing and Evaluation

The five anchor designs and tripod support structure were tested to determine their respective performance. By performing vertical pull tests on the anchors, actual uplift capacities could be compared with theoretical values. Field-tests were conducted on the tripod, on the research vessel, *R/V Gulf Challenger* to see if it was efficient in inserting the anchors. Initial response testing was performed on land. Field-testing of the anchors and tripod structure were conducted at five separate sites, each with individual sediment types.

Anchor Testing

The initial testing of the prototype cone anchor was performed in shallow water at the Jackson Research Laboratory. One reason for initially testing at this site was to validate the principles on which the hydro-jet anchor operates and to address any problems with the testing equipment (pump, hoses, etc). The water depth was approximately two feet. The sediment was composed primarily of clay with small stones. To perform the test, one member of the group assisted the insertion of the anchor by holding it vertical.

With the knowledge gained from the results of the initial test at the Jackson Research Laboratory, the cone anchor was field tested aboard the UNH research vessel, *R/V Gulf Challenger*. The test site, chosen by captains Paul Pelletier and Ken Houtler, is shown in Figure 14. The site is at the mouth of the Piscataqua River in approximately twenty feet of water.

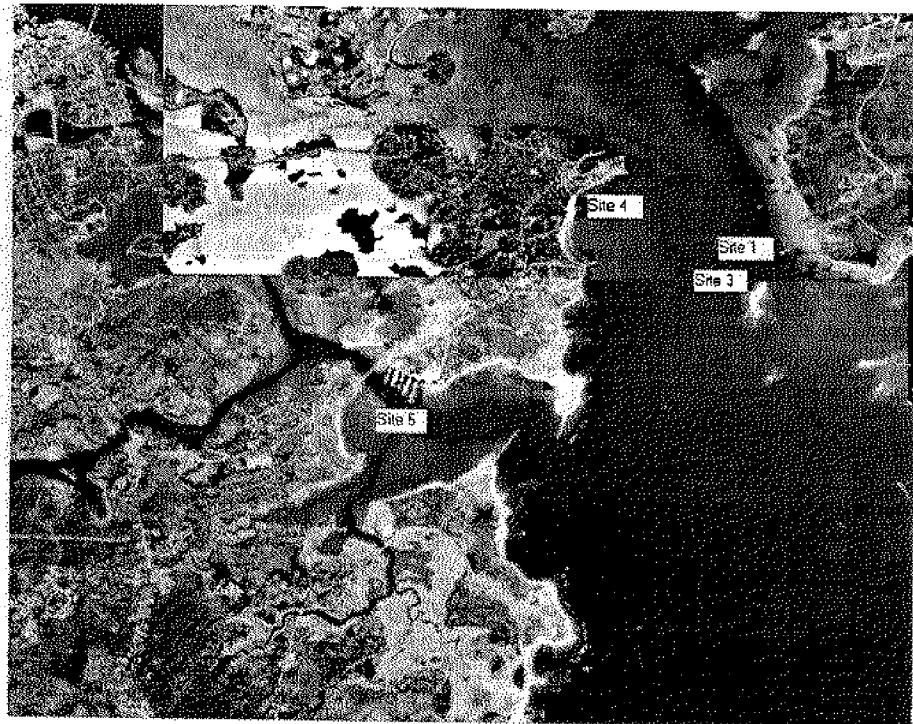


Figure 14: Map of test sites one, three, four, and five in Portsmouth harbor

First, a sediment sample was taken to determine the composition of the bottom. The sample proved to be coarse sand with no clay. Divers then took the anchor to the seafloor. The pump was activated, allowing the divers to insert the anchor. Once the anchor was in place the divers came to the surface to signal the deactivation of the pump. It took approximately three minutes to insert the anchor five feet into the sediment. The disturbed sediment was then allowed to settle for approximately fifteen minutes.

The vertical pull test on the inserted anchor was accomplished by first extending the A-frame on the stern of the *R/V Gulf Challenger* over the water. The towline attached to the anchor had been passed over the top of the A-frame before the anchor was inserted. A three thousand pound capacity winch onboard the *Challenger* provided the vertical lift. To begin the test, the aft of the boat was first pulled into position directly over the anchor using the winch. Once the boat was positioned, the towline was slackened to allow a five thousand pound capacity load-cell to be attached in line with the winch. Cinch arms were used to connect the load-cell inline with the towline.

The pull test was initiated by engaging the winch to attempt to pull the anchor out. A member of the team monitored the readout of load cell below deck during the pull test.

Surprisingly, the holding capacity of the anchor exceeded the capacity of the winch and thus stalled. The pump was reactivated to attempt to liquefy the sediment and thus reduce the pullout capacity of the anchor. However, while attempting to pull the anchor out resulted in breaking the shackle connecting the towline to the anchor. The divers inspected the anchor to determine if another connection could be made, but discovered the anchor had actually inserted itself deeper into the sediment when the pump was reactivated. The hose was cut and the team returned to land.

Tripod Testing

The tripod was initially tested on land to determine the performance of the triggering mechanism. The mechanism was set and the pump activated. The system worked approximately fifty percent of the time. One of the issues with the release mechanism's failure was that the flapper, which is inserted into the pipe, was too short. The flapper was redesigned so that it interfered with more of the flow in the pipe and thus producing a larger force required to trigger the pin. The holes in the pin guides were also increased in size to reduce their interference. The tripod was retested on land after the corrections were made. The redesigned elements improved its reliability to approximately ninety-eight percent.

Next, the tripod apparatus was tested in the UNH Ocean Engineering Offshore Basin. The trigger mechanism was set and the apparatus was lowered to the bottom of the tank. Once again, the trigger system worked dependably. Field-testing of the tripod was performed along with the redesigned anchors. The site of the second field test was located off the Isle of Shoals (Figure 15). The seabed consisted of clayey sand with amounts of shell and stone pieces. The wind and seas at the site were light.

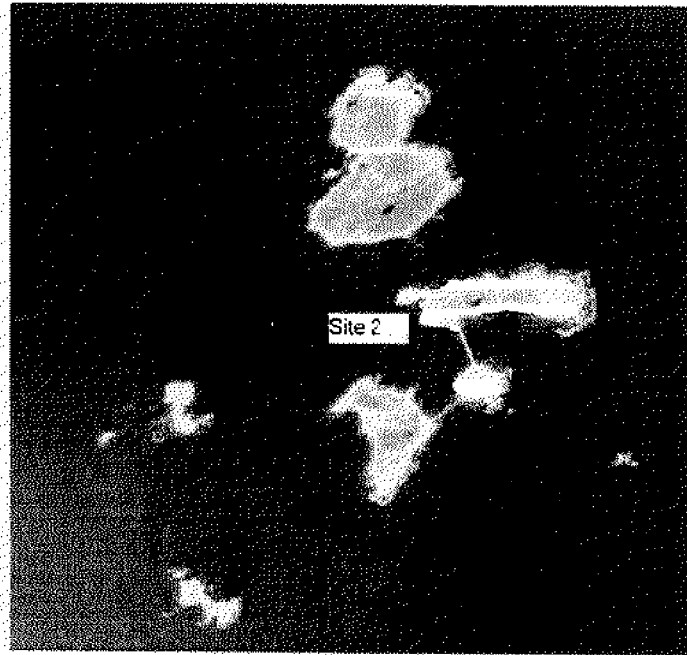


Figure 15: Second test site at the Isle of Shoals.

At the second test site, the smallest pyramid anchor was tested first. The tripod was used to insert the anchor. The anchor and tripod system were lowered from the A-frame using the capstan on the boat. Once the system reached the seabed, the pump was activated and once again, the release mechanism on the tripod performed well.

Due to the sediment type, the tripod was not able to insert the small anchor. In the best interests of the divers who were filming the operation of the system, the tripod was not used for the rest of the testing since maneuvering the tripod on deck required extended time. The testing continued using the medium sized anchor. This anchor was inserted using diver assistance to keep it vertical. Again, the sediment limited the embedment depth of the anchor to approximately one foot. This process took approximately ten minutes. After waiting twenty minutes, the sediment did not resettle over the anchor (see Figure 16), which resulted in the anchor becoming pulled out while trying to position the boat over the anchor. The sediment in this location contained too much clay and was too dense for the application of this anchor.

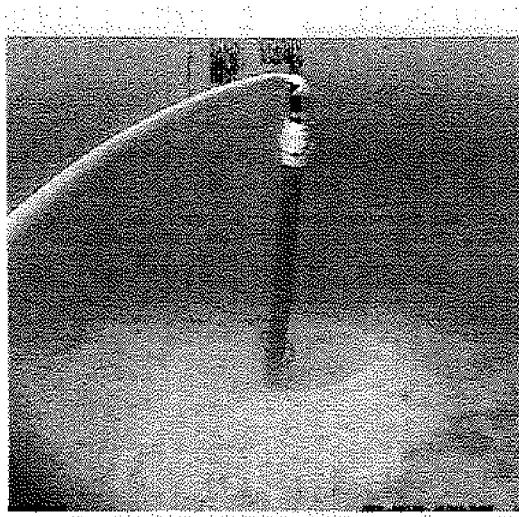


Figure 16: The anchor failed to embed itself after ten minutes of pumping water.

The third test site was located approximately three hundred yards from the first test site (more towards the center of the river) at the mouth of the Piscataqua River (see Figure 14). The sediment at this site was drastically different from that found at the first site despite its relative proximity. Its primary constituent was pea-sized cobblestone and thus the anchors could not penetrate.

The fourth test site was located next to the United States Coastguard station on the Piscataqua River (see Figure 14). The sediment was primarily fine sand with a slight clay constituent. A diver was able to insert the medium size anchor. The anchor was able to embed itself roughly thirty inches. While the sediment settled, the collapsible anchor was inserted with the same results. The sediment was allowed to settle for half an hour before the pull test was attempted. Both anchors pulled out while the boat was being positioned over the anchors. Upon further investigation it was determined the anchors pulled out because the sediment did not redeposit properly. A strong current in the test area carried the disturbed sediment from the anchors. In addition, the sediment was too dense and contained too much clay for the anchors application.

The last test site was conducted in Little Harbor (see Figure 14). The boat was tied to the float docks of the Wentworth Marina. The sediment was coarse sand, similar to that found on the first test site. In addition, there was very little current at the site. The large and medium size anchors were inserted without any occurrences. Each took approximately five minutes to embed itself twenty-five inches in the sediment. The sediment was allowed to settle for twenty minutes.

After the settling time was fulfilled, pull tests were conducted on the anchors that resulted in useable data. Time did not permit the vertical pull tests of the other two anchors.

Figure 17 shows the results after the large pyramid anchor was successfully inserted. Notice the relative cloudiness of the water due to the suspended sediments. Figure 18 shows the same anchor in Figure 17 after the suspended sediments had time to backfill. The resulting disturbed crater is approximately twenty-four inches in diameter.

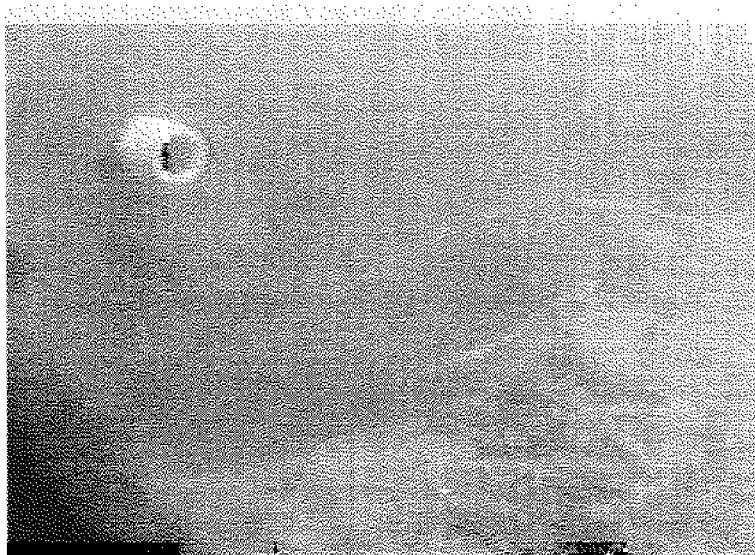


Figure 17: Anchor insertion process completed.



Figure 18: The resulting backfill of the sediment after a rest period of twenty minutes.

Results

The direct embedment anchors work best in sandy sediments that are easily liquefied by water pressure (Table 4). The water-jet action did not disturb the more dense soils like the fine sand/clay. Nor did it penetrate the pebble/sand sediment. The smallest anchor (two-inch pyramid) was initially used to test the different sediments.

Table 4: Relative successful embedding of the anchors in different sediments.

Sediment Type	Anchor Performance
Fine Sand/Clay	Limited Penetration
Coarse Sand	Complete Penetration
Pebble/Sand	No Penetration

Through the initial test performed at the Jackson Research Laboratory, it was observed that the hydro-jet action produced little upward thrust. One member of the group was more than capable of holding the anchor stationary. Therefore, it was determined that in later tests a diver could easily position the anchor without struggling against a thrust force. In addition, the weight of the tripod's insertion pole would provide a sufficient constant force to insert the anchors.

The tripod support system was successful in delivering the anchor to the sea floor. The release mechanism performed its operation of releasing the system. The structure was not used to insert the anchors in the testing following the second test site due to time constraints and diver safety.

The inability to retrieve the preliminary cone anchor from the first test site demonstrated that it was necessary for the depth of insertion to be limited so that the holding power of the anchor did not surpass the pulling capacity of the winch. Therefore, subsequent tests were performed based on a theoretical insertion limit determined from Figure 19, which was calculated using the largest anchor. A collar attached to the pipe of the tripod structure can be adjusted to vary insertion depths. In addition, the shanks of the anchors were limited to three feet.

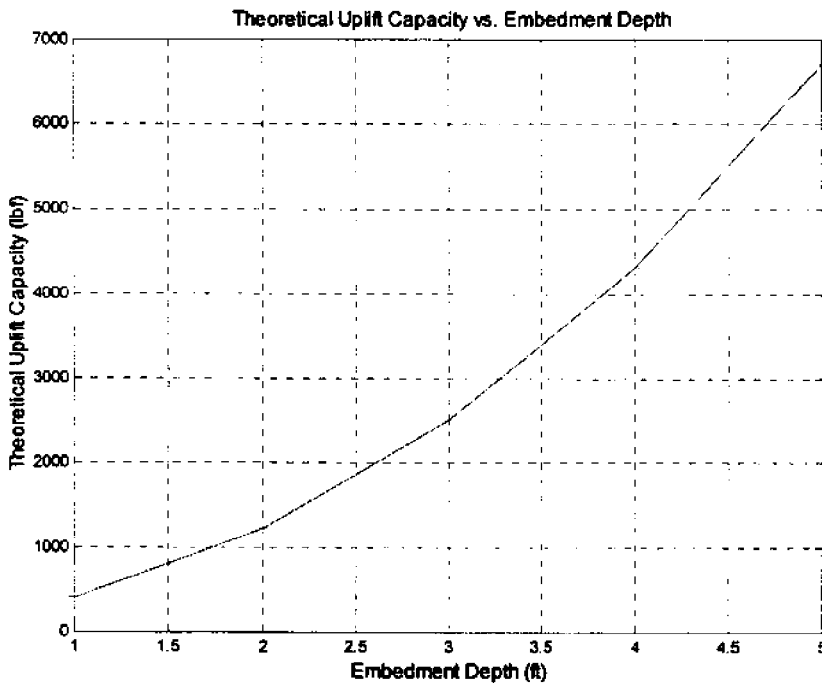


Figure 19: Theoretical uplift capacity versus anchor embedment depth.

The flexible high-pressure hose became crimped during the insertion process. Since the hose was connected in-line to the anchor or pipe, the crimping was due to the weight of the water in the hose. The crimping greatly influenced the flow rate through the hose and thus reduced the performance of the hydro-jet action. By attaching a ninety-degree elbow at the connection between the hose and pipe, the crimping issue was drastically reduced. This technique was used throughout the testing process.

During the insertion period, the anchors created craters that were approximately two feet in diameter (see Figure 17). A period between fifteen and twenty-five minutes was spent waiting after the insertion process finished to allow the sediment to resettle in the craters (see Figure 18).

The coarse sand sediment proved to be the most effective medium in which the anchors performed.

Table 5 shows the results of the pull test for three different anchors at semi-varying embedment depths. The theoretical and actual holding capacities are shown. Note that the actual holding capacity of the twelve-inch cone anchor is inconclusive since the winch used to perform the test has a working capacity of 3000 lbf. The winch stalled before the anchor could be pulled out.

Table 5: Experimental results of the anchor pull tests.

Anchor	Anchor Weight (lbf)	Test Site	Embedment Depth (in)	Sediment Type	Holding Capacity – Theoretical/Actual (lbf)
12-inch cone	25	1	84	Coarse Sand	6698/3300
12-inch pyramid	21.7	5	25	Coarse Sand	1310/640
6-inch pyramid	13.3	5	25	Coarse Sand	1019/326

Table 6 details the theoretical holding capacity to weight ratios of all the anchors that were fabricated. The actual ratios for those anchors that were tested are also shown. Figure 20 and Figure 21 graphically relate the theoretical and actual holding capacity to weight ratios of the tested anchors, respectively. Notice the actual ratio is approximately twice as small than that of the theoretical. In addition, the theoretical ratio has a trend opposite that of the actual ratio. The theoretical holding capacity to weight ratio increases as the size of the anchor decreases despite the first data point for the twelve-inch cone anchor. This trend is countered intuitive and its validity questioned by the actual data collected.

Table 6: Theoretical and actual holding capacity to weight ratios.

Anchor	Holding Capacity to Weight Ratio (Theoretical)	Holding Capacity to Weight Ratio (Actual)
12-inch cone	268	132
12-inch pyramid	60	29.5
6-inch pyramid (rigid)	77	24.5
6-inch pyramid (folding)	77	N/A
2-inch pyramid	84	N/A

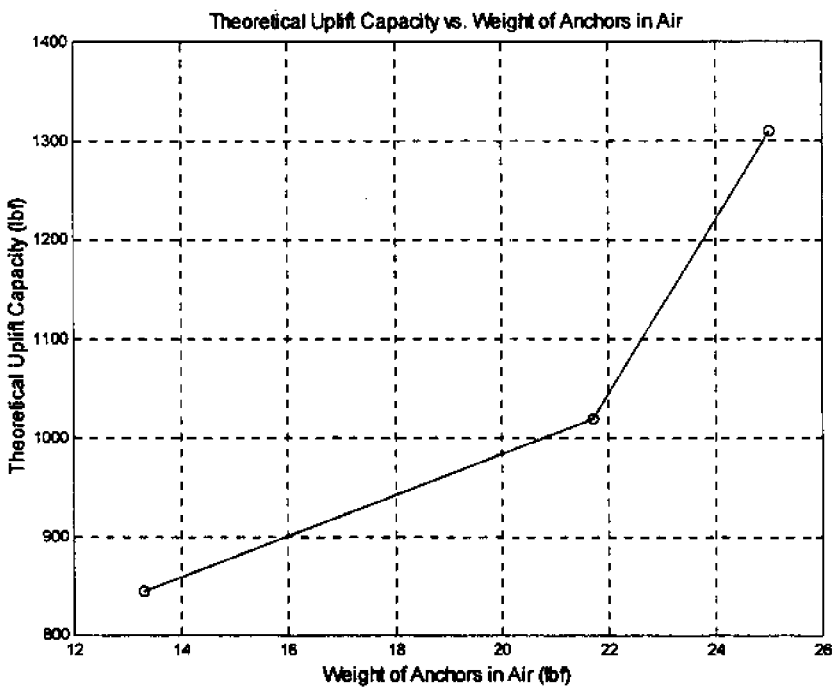


Figure 20: Theoretical uplift capacity versus weight of anchors in air.

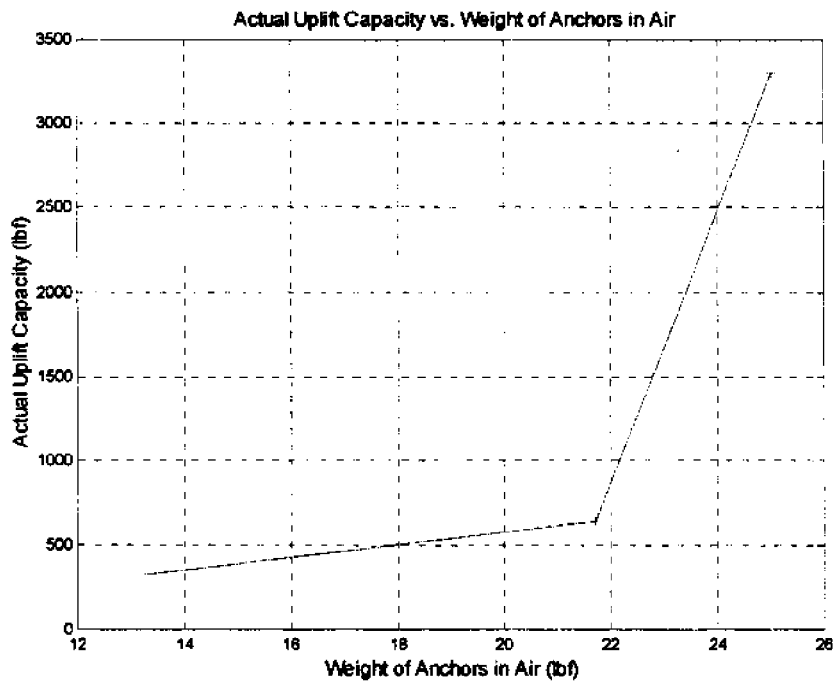


Figure 21: Actual uplift capacity versus weight of anchors in air.

Relationships can be drawn from the experimental data that validate the theoretical trends. Figure 22 shows a near-linear relationship between the theoretical holding capacity and the base area of the anchor. The test data for the large and medium pyramid anchors correspond to the same relationship (Figure 23). However, these are the only data points that can be compared due to the fact that these were the only two anchors that were tested at the same embedment depth and location. It is not possible to validate or disprove the theoretical calculations. The data that has been gathered indicates that the theoretical calculations are valid. A final conclusion can not be drawn without additional testing.

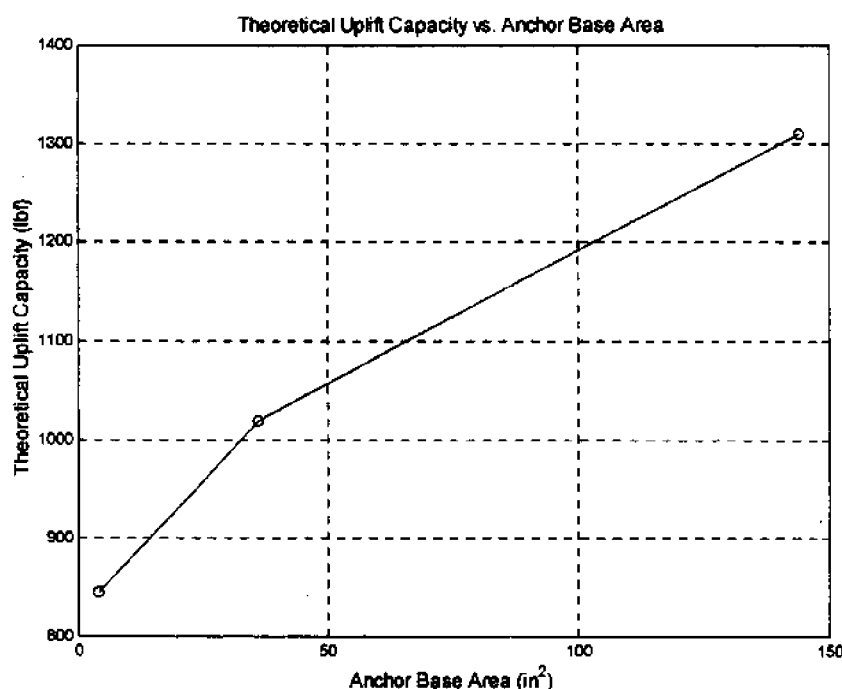


Figure 22: Theoretical uplift capacity versus anchor base area.

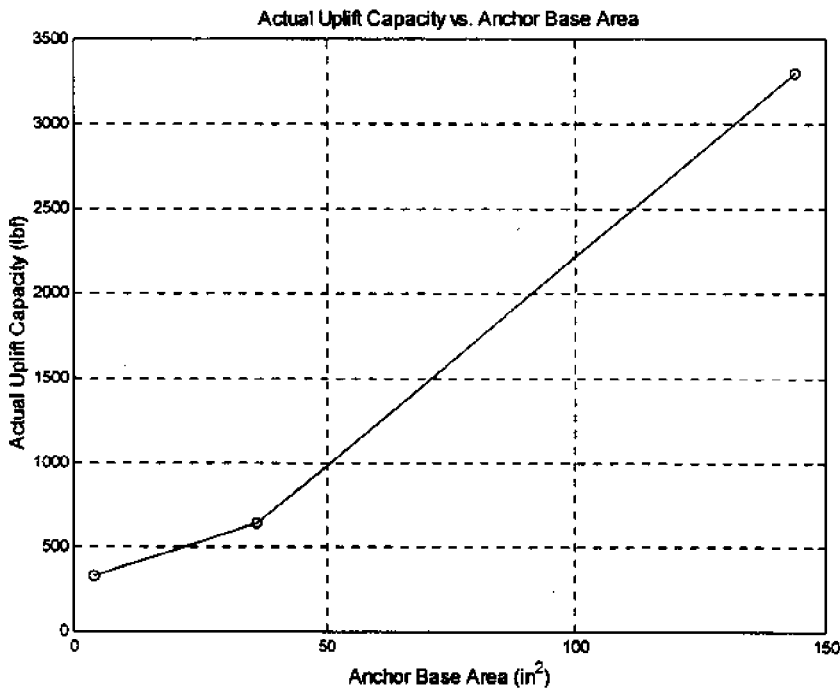


Figure 23: Actual uplift capacity versus anchor base area.

Discussion

Summary

The completed testing yielded valuable information concerning the application of the hydro-jet, direct embedment anchors and tripod insertion system. The hydro-jet anchor system is very substrate specific. Insertion of this anchor is very difficult unless performed in coarse sand. Being able to insert the anchor does not guarantee its performance. Once the anchor is inserted, the sediment must be allowed enough time for the suspended sediments and crater to cover over the anchor. Coarse sand is the ideal sediment that this anchor system will work.

Initial results do demonstrate the effectiveness of the anchor design. The general shape of the anchor gives a large holding capacity to weight ratio. However, the insertion depth plays a key role in the ultimate performance of the anchors. Initially, the cone anchor was inserted too deep whereas the subsequent anchors were inserted too shallow. The relationship between the insertion depth and sediment failure surface should be further researched.

The amount of time aboard the *R/V Gulf Challenger* was insufficient to complete the necessary tests to thoroughly analyze the system. The major difficulty was organizing a diver and simultaneously scheduling a boat date. Another limiting factor of the testing was the equipment available aboard the *R/V Gulf Challenger*. The winch aboard the vessel limited the size of the anchors that could be tested as well as the maximum embedment depth. A large capacity lift bag would solve this issue.

Future Testing

Before continuing the testing, several issues need to be addressed. First, the tripod insertion system should be redesigned so it can be maneuvered quickly and easily about the workboat. Making the design collapsible will assist its maneuverability.

Second, the release system is another area that requires tuning. The mechanical system is reliable; however, it permits substantial flow loss. Use of an electrical solenoid system that could trigger the release of the tripod pole and anchor from the surface could potentially neglect the need to cut a hole in the pole.

To improve the testing of the uplift capacity of the anchors, a lift bag should be used. A large capacity lift bag would allow the testing of larger anchors, thus increasing the range of data. The lift bag also allows other types of tests to be performed that are not possible with a

workboat. These tests include rapidly increasing loads and constant applied loads that would help investigate the affect of creep on the holding capacity.

Several test locations should be established in which to perform future tests. The sediment type, density, and other characteristics should be measured at the sites to ensure accurate results. The relationship between settling time, sediment density, and uplift capacity should be determined by inserting the anchors for extended periods to allow the sediment to return to a more natural density.

In addition, the four different sized anchors developed in this paper should be tested against one another in the test sites previously described. To ensure the validity of the data, each anchor should have at least three trials. Statistically, drawing an accurate relationship between the size of the anchor and its holding power depends on the amount of data collected.

A varying embedment depth test should also be performed with each anchor. To begin, each anchor should be inserted to the shallowest possible depth. Next, allow the sediment to return to as close to its natural density as possible and perform a pull test. Repeat the test with the anchor embedded one foot deeper. Continue this trend until significant data has been collected. The data should provide a more accurate representation of the relationship between the holding capacity and embedment depth.

It is not possible to validate or discredit the performance of the direct embedment, hydro-jet anchor design. Initial tests have demonstrated the system will work in specific sediment types. Further testing should be conducted to determine the limit of this type of anchor's capabilities in coarse sand sediment. Upon the completion of the testing, comparison of the data with other current anchoring systems ultimately will determine the performance of the hydro-jet anchor design.

References

Rocker, Karl Jr. "Handbook for Marine Geotechnical Engineering – Deep Ocean Technology" Naval Civil Engineering Laboratory; Port Hueneme, CA: 1985.

Appendix A: Theoretical uplift capacity calculations

Two sediment failure volume theories were used to predict the uplift capacity of the vertical lift anchors. The uplift capacity of the first anchor (cone shaped) was predicted using a cylindrical shear failure theory. Using this theory, the failure surface was predicted to be a right circular cylinder with the same diameter as that of the diameter of the cone. After analyzing the experimental data gained from testing the cone anchor, it was determined that the failure surface was a more complex shape. The subsequent anchors were built based on a failure surface that had a pyramid shape similar to the design of the anchors themselves.

Definition of Sediment Constants:

The approximate density and the friction angle of the sediment is given for coarse sand. These constants were approximated by Civil Engineering Professor, Pedro de Alba.

$$\gamma := 30 \cdot \frac{\text{lb}}{\text{ft}^3} \quad \text{Approximate density of sediment.}$$

$$\phi := 30 \cdot \text{deg} \quad \text{Friction angle of sediment.}$$

Definition of Variables:

The following variables will be used in the analysis of the cylindrical and pyramidal shear failure theories.

z - Depth the anchor is embedded in the sediment.

σ_{eff} - Effective normal stress due to the sediment.

τ - Effective shear stress due to the sediment.

R - Upper radius of the cone anchor.

S_{cone} - Surface area of the sediment failure surface.

F_{shear} - Force due to the shear on the walls of the sediment failure surface.

$F_{\text{total_uplift}}$ - Total uplift capacity of the anchor (including the mass of the sediment).

V_{cyl} - Volume of the sediment in the shear failure surface volume.

M_s - Mass of the sediment contained in the shear failure surface volume.

h - Height of anchor.

V_{cone} - Volume of failure surface.

θ - Angle between side of anchor and the vertical.

A - Base area of pyramid failure surface.

L_s - Base length of the sediment failure pyramid.

L - Base length of pyramid anchor.

V_{pyramid} - Volume of the sediment in the shear failure surface volume.

S_{pyramid} - Surface area of the sediment failure surface.

The cylindrical surface shear failure theory was used to predict the uplift capacity of the first cone anchor developed. The anchor's upper diameter is twelve inches and has a lower diameter of one inch. Using the cylindrical shear failure theory, τ takes into account the effective stress due to the sediment (σ_{eff}) and acts on the surface area of the cylinder. The calculations were performed for a design embedment depth of five feet.

$$z := 5 \cdot \text{ft} \quad \sigma_{\text{eff}} := \gamma \cdot z \quad \tau := (\sigma_{\text{eff}} \tan(\phi)) \cdot g$$

$$R := 6 \cdot \text{in} \quad \sigma_{\text{eff}} = 150 \frac{\text{lb}}{\text{ft}^2} \quad \tau = 0.601 \cdot \text{psi}$$

$$S := 2 \cdot \pi \cdot R \cdot z$$

$$S = 15.708 \text{ ft}^2 \quad F_{\text{shear}} := \tau \cdot S$$

$$F_{\text{shear}} = 1.36 \cdot 10^3 \cdot \text{lbf}$$

$$V_{\text{cyl}} := \pi \cdot R^2 \cdot z \quad M_s := \gamma \cdot V_{\text{cyl}} \quad W_s := M_s \cdot g$$

$$V_{\text{cyl}} = 3.927 \text{ ft}^3 \quad M_s = 117.81 \text{ lb} \quad W_s = 117.81 \cdot \text{lbf}$$

$$F_{\text{total_uplift}} := F_{\text{shear}} + W_s$$

$$F_{\text{total_uplift}} = 1.478 \cdot 10^3 \cdot \text{lbf}$$

Through testing, it was determined that these calculations were too conservative (see Results and Discussion section). Therefore, a second shear failure surface theory was used to design the subsequent anchors. This calculation for the uplift capacity of the anchors was performed using a sediment failure surface that was the same shape as the anchors. The final shape of the anchors was ultimately determined by the cost of manufacturing. The cost to fabricate pyramid shaped anchors was several thousand dollars less than the cost to fabricate cone anchors. Therefore, the theoretical uplift calculations were performed assuming a pyramidal failure surface.

To develop the dimensions of the anchors, an iteration was performed to determine the maximum embedment depth of the largest of the anchors (twelve inch square upper area). Next, a second iteration was performed to determine a range of dimensions for three anchors at the chosen embedment depth.

$$\begin{aligned}
 z &:= \begin{bmatrix} 1 \\ 2 \\ 3 \\ 4 \\ 5 \end{bmatrix} \text{ ft} & L &:= 12 \text{ in} \\
 \theta &:= 24.6 \text{ deg} \\
 h &:= 12 \text{ in} \\
 L_s &:= L + 2 \cdot z \cdot \tan(\theta) & A &:= L_s^2 & V_{\text{pyramid}} &:= \frac{1}{3} \cdot (A \cdot (h + z)) & S_{\text{pyramid}} &:= 4 \cdot \left(\frac{1}{2} \cdot (L_s \cdot z) \right) \\
 L_s &= \begin{bmatrix} 1.916 \\ 2.831 \\ 3.747 \\ 4.663 \\ 5.578 \end{bmatrix} \text{ ft} & A &= \begin{bmatrix} 3.67 \\ 8.017 \\ 14.04 \\ 21.741 \\ 31.118 \end{bmatrix} \text{ ft}^2 & V_{\text{pyramid}} &= \begin{bmatrix} 2.447 \\ 8.017 \\ 18.72 \\ 36.234 \\ 62.236 \end{bmatrix} \text{ ft}^3 & S_{\text{pyramid}} &= \begin{bmatrix} 3.831 \\ 11.325 \\ 22.482 \\ 37.301 \\ 55.784 \end{bmatrix} \text{ ft}^2 \\
 M_s &:= \gamma \cdot V_{\text{pyramid}} & W_s &:= M_s \cdot g & F_{\text{shear}} &:= \tau \cdot S_{\text{pyramid}} & F_{\text{total_uplift}} &:= F_{\text{shear}} + W_s \\
 M_s &= \begin{bmatrix} 73.396 \\ 240.495 \\ 561.605 \\ 1.087 \cdot 10^3 \\ 1.867 \cdot 10^3 \end{bmatrix} \text{ lb} & W_s &= \begin{bmatrix} 73.396 \\ 240.495 \\ 561.605 \\ 1.087 \cdot 10^3 \\ 1.867 \cdot 10^3 \end{bmatrix} \text{ lb} & F_{\text{shear}} &= \begin{bmatrix} 331.804 \\ 980.806 \\ 1.947 \cdot 10^3 \\ 3.23 \cdot 10^3 \\ 4.831 \cdot 10^3 \end{bmatrix} \text{ lbf} & F_{\text{total_uplift}} &= \begin{bmatrix} 405.2 \\ 1.221 \cdot 10^3 \\ 2.509 \cdot 10^3 \\ 4.317 \cdot 10^3 \\ 6.698 \cdot 10^3 \end{bmatrix} \text{ lbf}
 \end{aligned}$$

The maximum embedment depth is chosen to be three feet.

The dimensions of the pyramid anchors were designed to remain proportional to each other. Thus, the base length of the anchors was changed and subsequently, the height also changed to maintain a one to one ratio.

$$z := 25 \text{ in}$$

$$L := \begin{bmatrix} 2 \\ 6 \\ 12 \end{bmatrix} \text{ in} \quad h := \begin{bmatrix} 2 \\ 6 \\ 12 \end{bmatrix} \text{ in}$$

$$L_s := L + 2 \cdot z \cdot \tan(\theta) \quad A := L_s^2$$

$$L_s = \begin{bmatrix} 2.074 \\ 2.408 \\ 2.908 \end{bmatrix} \text{ ft} \quad A = \begin{bmatrix} 4.303 \\ 5.797 \\ 8.454 \end{bmatrix} \text{ ft}^2$$

$$V_{\text{pyramid}} := \frac{1}{3} \cdot (A \cdot (h + z))$$

$$V_{\text{pyramid}} = \begin{bmatrix} 3.227 \\ 4.992 \\ 8.689 \end{bmatrix} \text{ ft}^3$$

$$S_{\text{pyramid}} := 4 \cdot \left(\frac{1}{2} \cdot (L_s \cdot z) \right)$$

$$S_{\text{pyramid}} = \begin{bmatrix} 8.643 \\ 10.032 \\ 12.115 \end{bmatrix} \text{ ft}^2$$

$$M_s := \gamma \cdot V_{\text{pyramid}}$$

$$W_s := M_s \cdot g$$

$$F_{\text{shear}} := \tau \cdot S_{\text{pyramid}}$$

$$F_{\text{total_uplift}} := F_{\text{shear}} + W_s$$

$$M_s = \begin{bmatrix} 96.813 \\ 149.75 \\ 260.678 \end{bmatrix} \text{ lb}$$

$$W_s = \begin{bmatrix} 96.813 \\ 149.75 \\ 260.678 \end{bmatrix} \text{ lbft}$$

$$F_{\text{shear}} = \begin{bmatrix} 748.504 \\ 868.785 \\ 1.049 \cdot 10^3 \end{bmatrix} \text{ lbft}$$

$$F_{\text{total_uplift}} = \begin{bmatrix} 845.317 \\ 1.019 \cdot 10^3 \\ 1.31 \cdot 10^3 \end{bmatrix} \text{ lbft}$$

Appendix B: Pressure loss in water hose.

Energy Equation for a Real Fluid

$$\frac{P_1}{\rho} + g \cdot z_1 + \frac{V_1^2}{2} = \frac{P_2}{\rho} + g \cdot z_2 + \frac{V_2^2}{2} + h_f$$

P = pressure at section

z = the vertical distance from a datum to the sections (the potential energy)

V = average velocity of the fluid at the sections

g = acceleration of gravity

ρ = the density of the fluid

h_f = the head loss (friction)

Head Loss

$$h_f = f \cdot \frac{L \cdot V^2}{D \cdot 2g}$$

f = f(Re, e/D), the friction factor

D = diameter of hose

L = length over which the pressure drop occurs

e = roughness factor

Reynolds Number

$$Re = \frac{\rho \cdot V \cdot D}{\mu}$$

μ = dynamic viscosity

Define known variables

$$\rho := 1025 \frac{\text{kg}}{\text{m}^3} \quad g := 9.81 \frac{\text{m}}{\text{sec}^2} \quad D := 1.5 \cdot \text{in}$$

$$\mu := .00108 \frac{\text{newton} \cdot \text{sec}}{\text{m}^2} \quad z_1 := 0 \cdot \text{ft}$$

Variables picked or estimated

$$z_2 := 0 \cdot \text{ft}, 1 \cdot \text{ft}, 200 \cdot \text{ft} \quad L(z_2) := z_2 - z_1$$

$$P_1 := 100 \cdot \text{psi}$$

Estimate V from flow rate of 20 gal/min

$$\text{vol} = \pi \cdot r^2 \cdot l$$

$$\text{vol} := 20 \cdot \text{gal} \quad r := \frac{D}{2}$$

$$l := \frac{\text{vol}}{\pi \cdot r^2} \quad l = 217.865 \text{ ft}$$

$$20 \frac{\text{gal}}{\text{min}} \quad \rightarrow \quad V := 217.865 \cdot \frac{\text{ft}}{\text{min}}$$

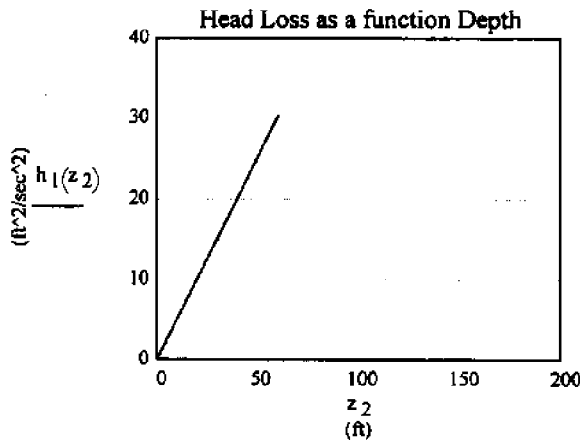
$$Re := \frac{\rho \cdot V \cdot D}{\mu}$$

$$Re = 4.002 \cdot 10^4$$

$$\text{Assume} \quad e := .0005 \cdot \text{ft} \quad \frac{e}{D} = 4 \cdot 10^{-3}$$

$$f = f\left(Re, \frac{e}{D}\right) \quad \text{From Moody (Stanton) Diagram} \quad f := .031$$

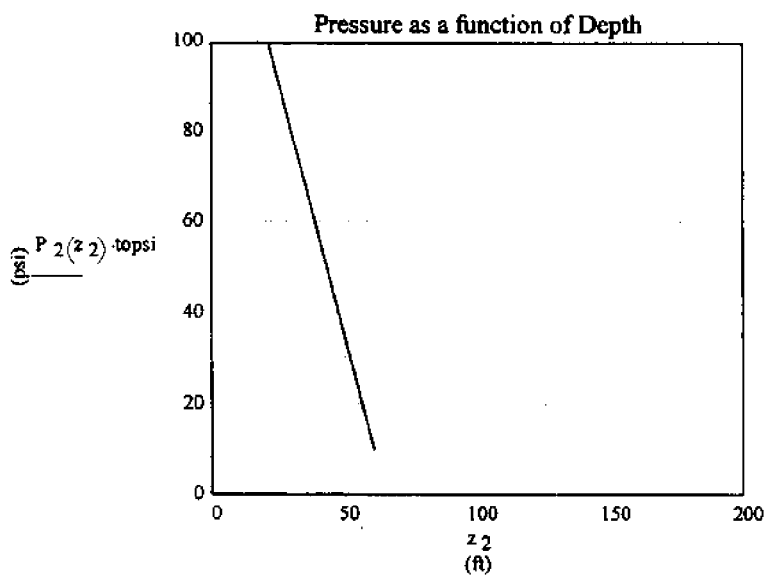
$$h_1(z_2) := f \cdot \frac{L(z_2)}{D} \cdot \frac{V^2}{2}$$



$$\frac{P_1}{\rho} + g \cdot z_1 + \frac{V_1^2}{2} = \frac{P_2}{\rho} + g \cdot z_2 + \frac{V_2^2}{2} + h_1$$

Assume $V = \text{constant}$ (cancels) and solve for P_2

$$P_2(z_2) := \left(\frac{P_1}{\rho} + g \cdot z_1 - g \cdot z_2 - h_1(z_2) \right) \cdot \rho$$



$$P_2(25 \text{ ft}) = 88.323 \text{ psi}$$

$$P_2(50 \text{ ft}) = 76.645 \text{ psi}$$

$$P_2(75 \text{ ft}) = 64.968 \text{ psi}$$

$$P_2(100 \text{ ft}) = 53.29 \text{ psi}$$

$$P_2(125 \text{ ft}) = 41.613 \text{ psi}$$

$$P_2(150 \text{ ft}) = 29.935 \text{ psi}$$

$$P_2(175 \text{ ft}) = 18.258 \text{ psi}$$

$$P_2(200 \text{ ft}) = 6.58 \text{ psi}$$

